XIV. International Conference on
Nuclear Structure Properties
Selcuk University, Konya, Turkey
(3 June, 2021)

CLUSTERING PHENOMENON İN THE DECAY OF LİGHT MASS COMPOSİTE NUCLEI

Prof. (Dr.) BirBikram Singh
drbirbikramsingh@gmail.com

DEPARTMENT OF PHYSICS
AKAL UNIVERSITY
Talwandi Sabo-151302, Bathinda, Punjab (India)

SELCUK UNIVERSITY
FACULTY OF SCIENCE

XIV. International Conference On Nuclear Structure Properties

We are pleased to announce the XIV. International Conference on Nuclear Structure Properties, NSP2021 to be held as online meeting on 2-4 June 2021 in Selcuk University, Konya, TURKEY.

2- 4 June 2021

Conference web page: http://nsp2021.selcuk.edu.tr

Clustering in Universe

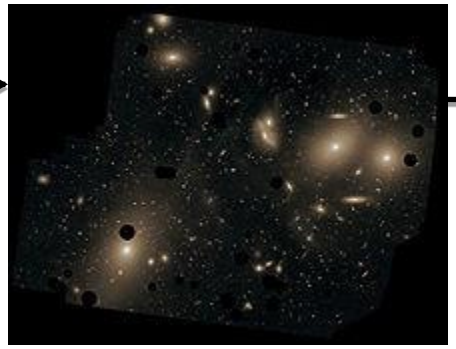

Galaxy Clusters

Star Clusters

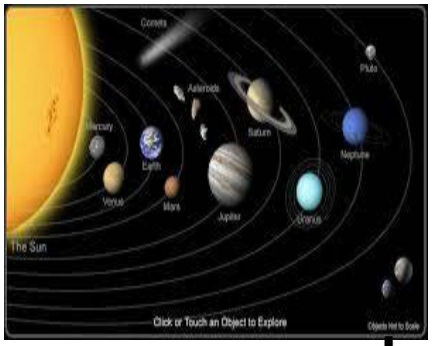

Planets

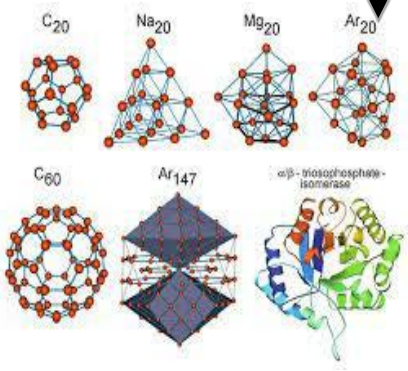

Atom Clusters

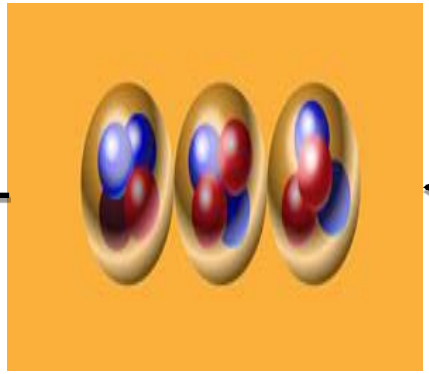

Alpha Clusters

Nucleus?

If not, surprising!!

Proton Neutron Clusters

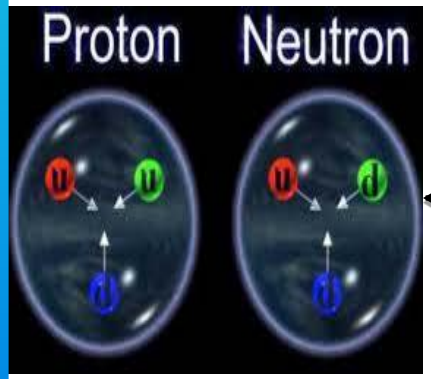

Quark Clusters

Subject of clustering transcends many areas of science, from clusters of galaxies to clusters of micro-organisms, which obviously encompasses atomic, nuclear and sub-nuclear domains also [***W. Greiner, Z. Phys. A 349, 315 (1994)***].

❖The discovery of alpha (α) decay in the heavy nuclei prompted the idea that nucleus can be visualized as being composed of α particles as building block [G. Gamow, Z. Phys. A **51**, 204 (1928)].

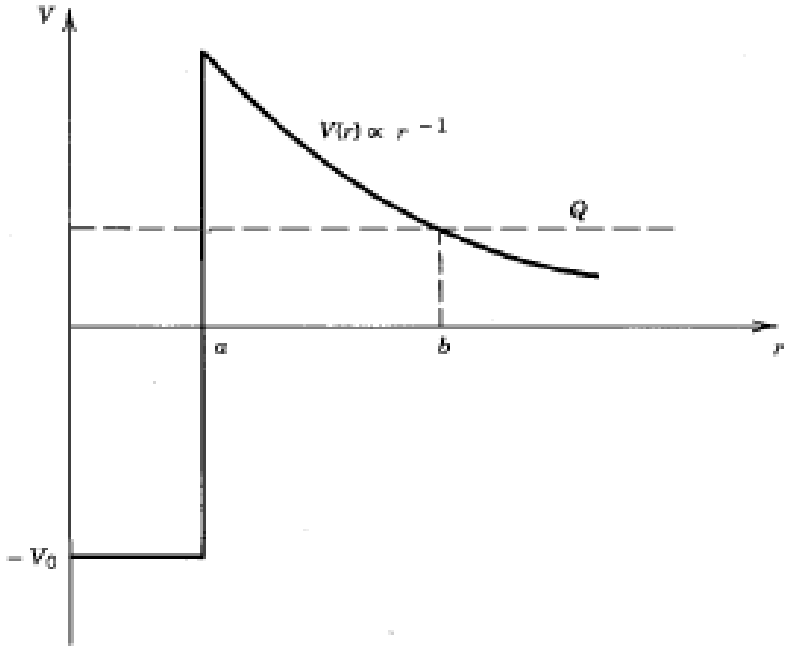

Figure 8.3 Relative potential energy of α-particle, daughter-nucleus system as a function of their separation. Inside the nuclear surface at $r = a$, the potential is represented as a square well; beyond the surface, only the Coulomb repulsion operates. The α particle tunnels through the Coulomb barrier from a to b.

❖ The α clustering, specifically in the light alpha conjugate nuclei with N=Z has been examined extensively. The famous 'Hoyle state' i.e. ^{12}C consisting of three alpha particles was predicted theoretically in 1953 [F. Hoyle et al., Phys. Rev. **92**, 1095 (1953)] and later on found experimentally in 1957 [C.W. Cook et al., Phys. Rev. **107**, 508 (1957)].

❖Ikeda suggested that these alpha cluster states are not predominant in the ground state but manifest near the cluster decay threshold energies [Ikeda et al., Prog.Theor. Phys. Suppl. E **68**, 464 (1968)].

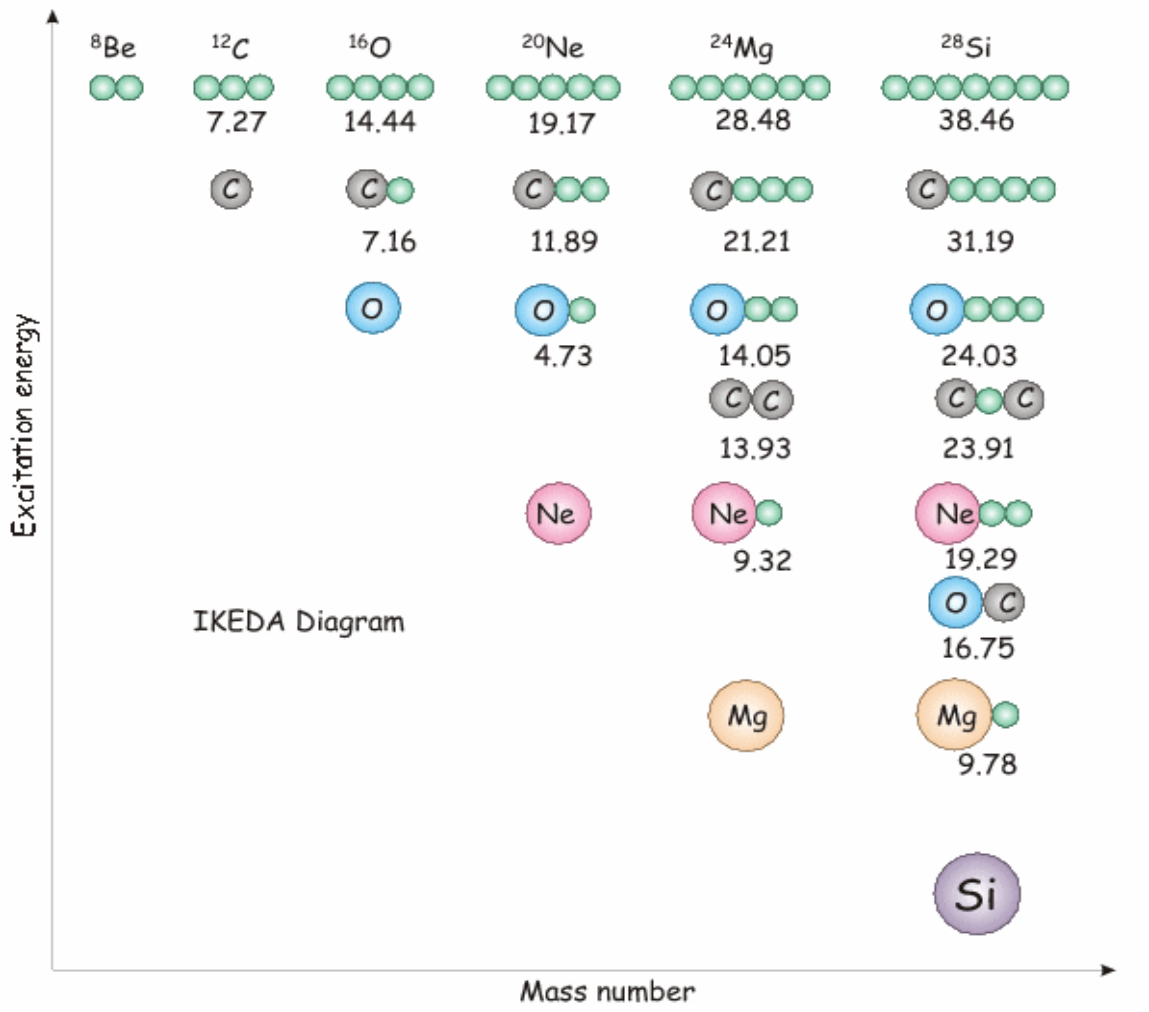

Fig: Ikeda threshold diagram for N=Z (or nα) nuclei

❖Oertzen et al. extended the work of alpha cluster structure of Ikeda, to the case of the light neutron rich nuclei and proposed that these nuclei can be speculated as alpha core with valence neutrons [Oertzen et al., Eur. Phys. J. A **43**, 17 (2010)].

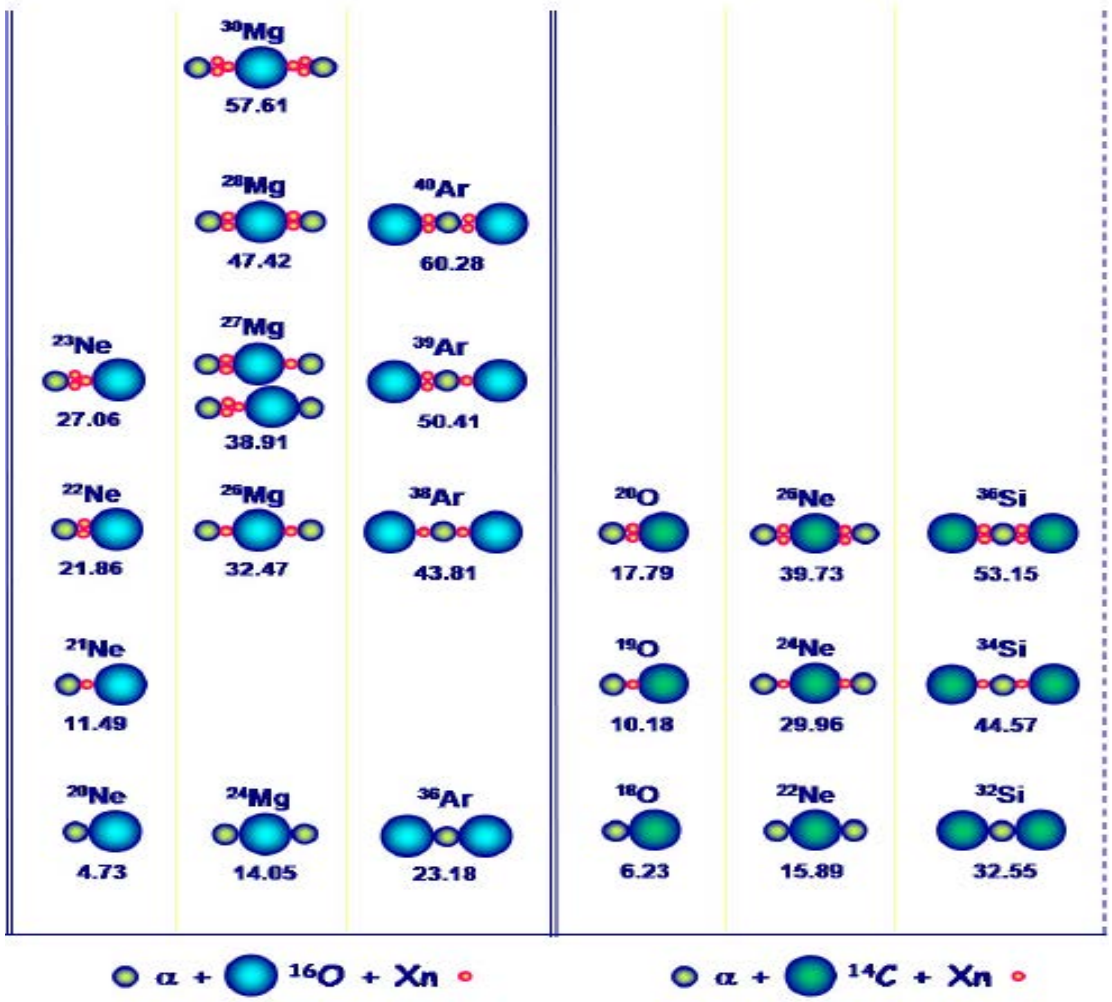

Fig: Modified Ikeda diagram showing molecular structures and the associated excitation energy.

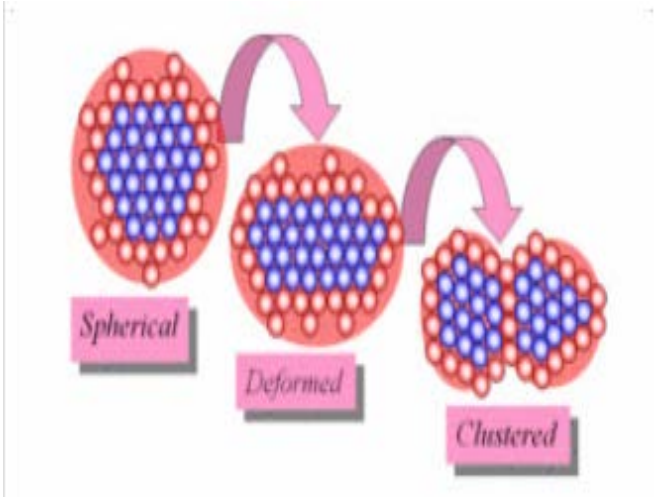

Fig: Pictorial representation of energetic advantage of clustering for nuclear matter at neutron drip line in order that valence neutrons (red) can maximize their interaction with the core nucleons (blue).

- In nuclear dynamics, as seen in light stable nuclei, clustering is one of the essential features and various cluster structures have been known even in the low-energy region.

- Also, in the physics of unstable nuclei, clustering features comprise one of the central subjects.

- It is already well known [***Y. Kanada-En'Yo, M. Kimura, and H. Horiuchi, C. R. Phys. 4, 497 (2003) and earlier references therein***] that clustering structures appear in the ground states of light nuclei with $N=Z$ or in their neighborhood.

- When cluster structures are prominent, the description by conventional mean-field models based on the shell-model-like picture becomes insufficient.

- Fortunately, the properties of light nuclei with cluster structures have been well studied with cluster models where the existence of clusters is assumed *a priori*.

- This assumption, however, sets a limitation for applying the cluster models to “exotic” (unstable) nuclei, where structural information is rather scanty.

- Thus, a model that could explain both the mean-field and clustering properties of nuclei would be helpful to obtain a systematic understanding of both the stable and exotic nuclei.

- Examples of such successful frameworks are the methods of Fermionic molecular dynamics (FMD) [*H. Feldmeier and J. Schnack, Rev. Mod. Phys.* ***72****, 655 (2000)*] and antisymmetrized molecular dynamics (AMD) [Y. Kanada-En’Yo and H. Horiuchi, Prog. Theor. Phys. Suppl. **142**, 205 (2001)].

- Both of which describe well the structural properties of several nuclei and their excited states, in the lighter mass region.

- Another model, which is capable of explaining the clustering shapes in light nuclei is the relativistic mean field theory (RMFT) [***S. K. Patra, C.-L. Wu, C. R. Praharaj, and R. K. Gupta, Nucl. Phys. A651, 117 (1999)***].
- This theory has been successfully applied to nuclei throughout the nuclear chart and, with some extensions, also to nuclear matter and neutron stars.

PHYSICAL REVIEW C **71**, 064308 (2005)

Relativistic mean field study of clustering in light nuclei

P. Arumugam, B. K. Sharma, and S. K. Patra
Institute of Physics, Sachivalaya Marg, Bhubaneswar-751 005, India

Raj K. Gupta*
Department of Physics, Panjab University, Chandigarh-160 014, India

- **In this work, for the first time the applicability of the RMFT was explored for explaining the possible cluster structures in lighter mass stable and exotic nuclei.**

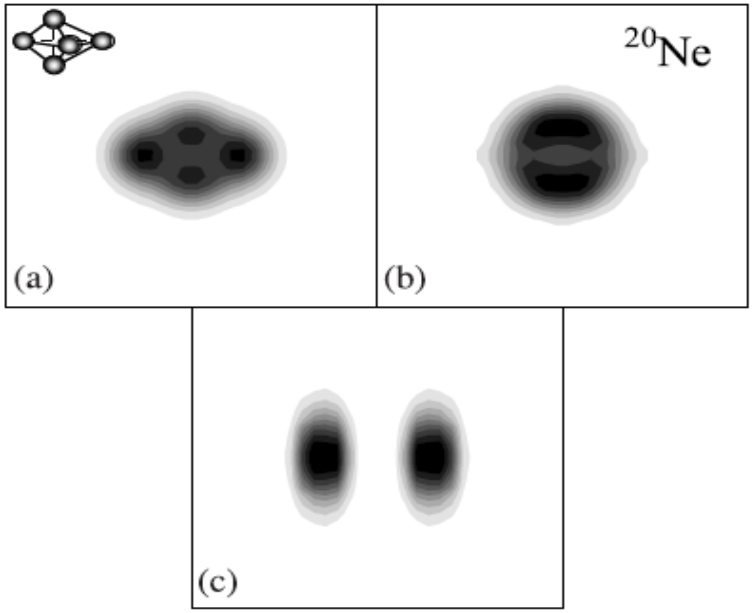

FIG. 7. Matter density distribution in ^{20}Ne.

Nucleus	B.E. (MeV)		β_2		Probable structure
	Theor.	Expt.	Theor.	Expt.	
^{20}Ne	156.70	160.64	0.54	0.73	5α—trigonal bipyramid
	151.96		–0.24		^{10}B + ^{10}B
	108.24		7.76		^{10}B + ^{10}B—(fragments)

PHYSICAL REVIEW C 74, 044311 (2006)

α-cluster structure and exotic states in a self-consistent model for light nuclei

ELSEVIER

Available online at www.sciencedirect.com

ScienceDirect

Physics Reports 432 (2006) 43–113

PHYSICS REPORTS

www.elsevier.com/locate/physrep

Nuclear clusters and nuclear molecules

W. von Oertzen[a, b], Martin Freer[c, *], Yoshiko Kanada-En'yo[d]

PHYSICAL REVIEW C **83**, 034312 (2011)

Localization in light nuclei

P.-G. Reinhard,[1] J. A. Maruhn,[2] A. S. Umar,[3,*] and V. E. Oberacker[3]

How atomic nuclei cluster

J.–P. Ebran[1], E. Khan[2], T. Nikšić[3] & D. Vretenar[3]

NATURE | VOL 487 | 19 JULY 2012

doi:10.1038/nature11246

❖Nucleonic matter — the protons and neutrons that comprise atomic nuclei — acts predominantly as a quantum liquid, but lighter nuclei behave more like molecules composed of clusters of protons and neutrons.

❖Clustering is related to the overall nuclear interaction, but its detailed mechanism is not fully understood.

❖These authors use theoretical modeling to calculate the conditions that cause clustering in ^{20}Ne, a small nucleus thought to favor clustering.

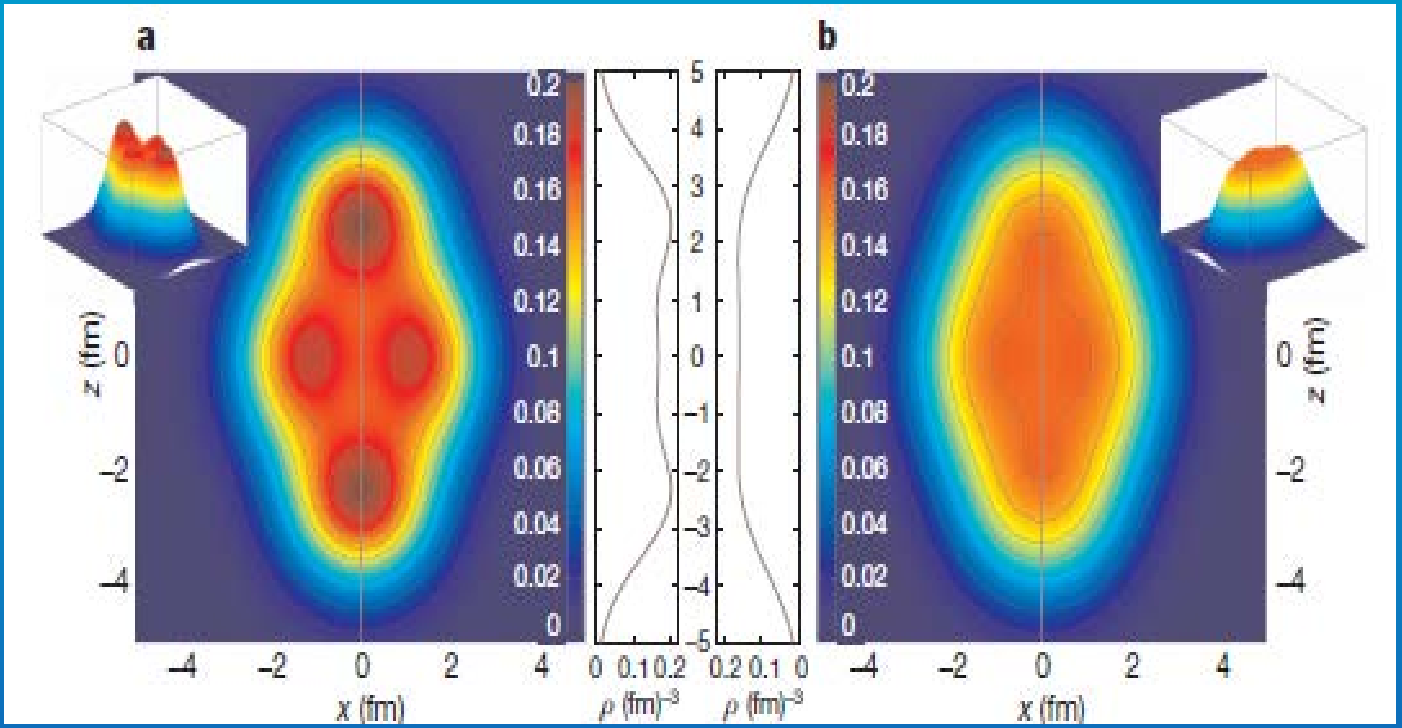

Figure 1 | Self-consistent ground-state densities of ^{20}Ne. Two nuclear energy-density functionals are used: **a**, DD-ME2 (ref. 22), and **b**, Skyrme SLy4 (refs 21 and 30). The densities (in units of fm^{-3}) are plotted in the $x-z$ plane of the intrinsic frame of reference that coincides with the principal axes of the nucleus, with z chosen as the symmetry axis. The inserts show the corresponding three-dimensional density plots and the density profiles (ρ) along the symmetry axis ($x = 0$).

❖The density calculated with SLy4 displays a smooth behavior characteristic of a Fermi liquid, with an extended surface region in which the density very gradually decreases from the central value of around 0.16 fm^{-3} (Fig. 1b).

❖The relativistic functional DD-ME2, on the other hand, predicts an equilibrium density that is much more localized. The formation of cluster structures is clearly visible, with density spikes as large as roughly 0.2 fm^{-3}, and a much narrower surface region (Fig. 1a).

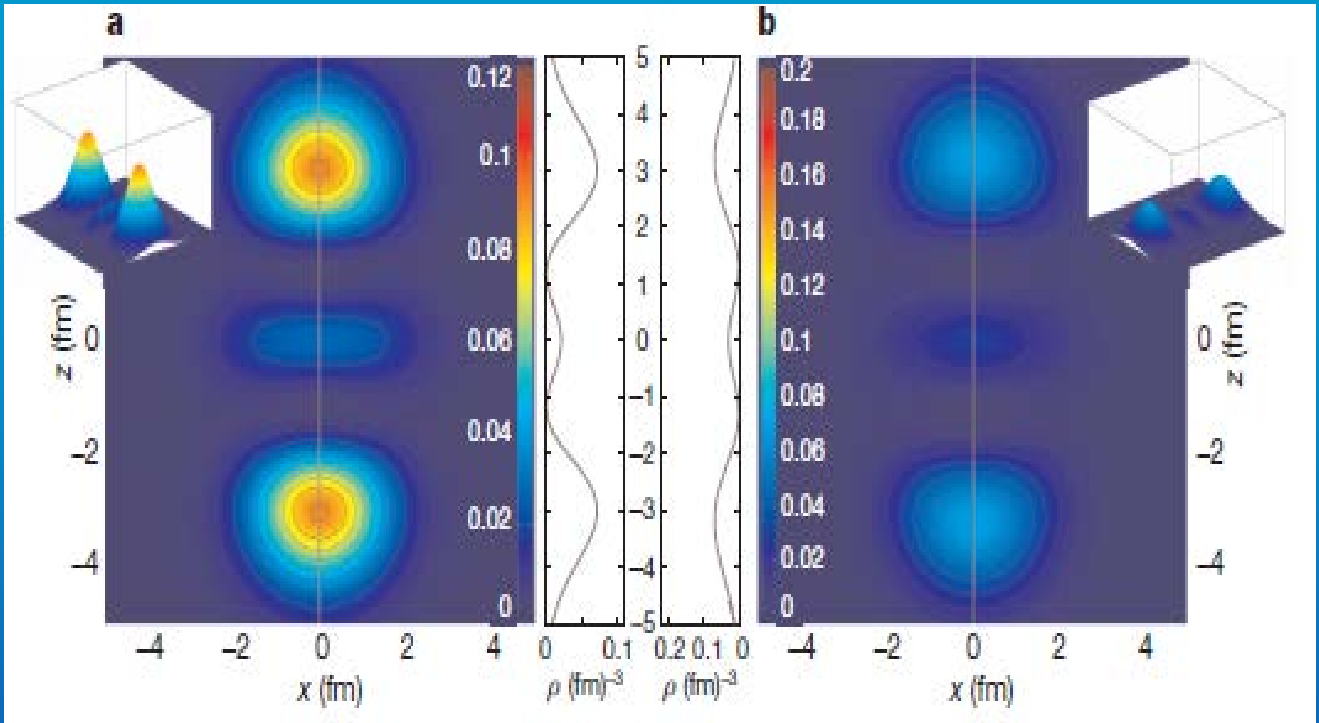

Figure 2 | Partial nucleon density distributions. Density distributions that correspond to the highest occupied level (2 protons spin up and down, and 2 neutrons spin up and down) in ^{20}Ne, having Nilsson quantum numbers $1/2^{+}[220]$, calculated using the nuclear energy-density functionals DD-ME2 (ref. 22) (**a**) and SLy4 (refs 21 and 30) (**b**).

- **DD-ME2 predicts a much more localized density distribution (Fig. 2a)**
- **Localization of densities that correspond to single-particle orbital is a necessary precondition for the formation of clusters.**

❖ The cluster structures are predicted in the case of alpha and non-alpha conjugate nuclei from ^{8}Be to ^{40}Ca [Yahmaya et al., Phys. Lett. B **306**, 1 (1993); M Freer, A C Merchant, J. Phys. G: Nucl. Part. Phys. **23**, 261 (1997); G. V. Rogachev et al., PRC **64**, 051302(R) (2001]. Experimentally, the cluster structures are probed through cluster knock out, capture reactions etc. [R.K. Sheline et al., Nucl. Phys. **21**, 196 (1960); F.D. Becchetti et al., Nucl. Phys. A **339**, 132 (1980); D. Jenkins, J. Phys. Conf. Series **436**, 012016 (2013)].

❖**The heavy ion reactions at low energy are useful tool** to study the cluster structure of decaying composite nucleus formed during the course of reaction. Several attempts have been made to explore the role of clustering on the reaction mechanism of alpha conjugate systems i.e. ^{16}O+^{12}C,^{20}Ne+^{12}C, ^{28}Si+^{12}C etc. [K. Daneshvar et al., PRC **25**, 1342 (1982); D. Shapira et al., Phys. Lett. **114B**, 111 (1982); A. Dey et al., PRC **76**, 034608 (2007); S. Kundu et al., PRC **78**, 044601 (2008)].

❖During last decades, the decay of several light and medium mass nuclei with mass~ 20-40 have been studied to explore the reaction mechanisms. It is interesting to explore the clustering effects in the decay of composite systems formed in heavy ion reactions.

❖The decay of composite systems with the mass varying from light to heavy, super heavy regions have been studied successfully within the collective clusterization process of dynamical cluster decay model (DCM) [R.K. Gupta et al., PRC **68,** 014610 (2003); Lecture Notes in Physics, Clusters in nuclei, edited by C. Beck, **818**, 223 (2010)].

❖DCM is based upon the well established quantum mechanical fragmentation (QMFT) theory. The QMFT based study supports the ^{14}C clustering in ^{18,20}O, ^{22}Ne systems with inclusion of modified temperature dependent pairing strength δ(T) in the liquid drop energies [M. Bansal et al., J. of Phys. Conf. Series **321,** 012046 (2011)].

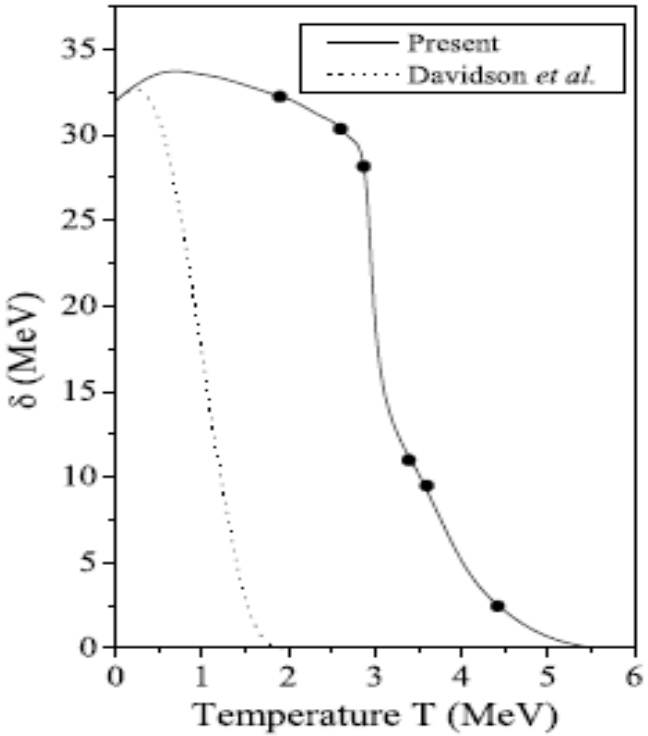

➢Fig: The variation of pairing constant with temperature obtained from QMFT based model [R. K. Gupta et al., Int. Rev. Phys. **2**, 369 (2008)] calculations, compared with that used by Davidson et al. [N. J. Davidson et al., Nucl. Phys. A **570**, 61c (1994)]

❖**Here**, the clustering effects in light mass N=Z ($^{20}Ne^{*}$, $^{28}Si^{*}$,$^{40}Ca^{*}$) and N≠Z composite systems ($^{21,22}Ne^{*}$, $^{39}K^{*}$) formed in low energy heavy ion reactions at different excitation energies, within the collective clusterization approach of the dynamical cluster-decay model (DCM) based on quantum mechanical fragmentation theory (QMFT), are presented.

❖ A comparative decay analysis of these systems has been undertaken for the emission of different intermediate mass fragments (IMFs)/clusters, specifically the IMFs having Z=3, 4 and 5 (or Z=7, 6 and 5 complimentary fragments from the $^{20}Ne^{*}$ and $^{21,22}Ne^{*}$ composite systems) which are having the experimental data available for their Z-distribution [M.M. Coimbra et al., NPA **535,** 161 (1991); S. Kundu et al., PRC 85, 064607 (2012); Parmana J. Phys. 82, 727 (2014)].

❖The study reveals the presence of competing reaction mechanisms of compound nucleus (fusion-fission, FF) and of non-compound nucleus origin (deep inelastic orbiting, DIO) in the decay of very light mass composite systems $^{20,21,22}Ne^{*}$ and $^{28}Si^{*}$ at different excitation energies

Methodology

- To study ground state emissions of nucleus and emissions of excited compound nucleus (CN) in heavy ion reactions, Gupta and collaborates developed the dynamical (or quantum mechanical) fragmentation theory, in the form of **PCM** and **DCM**, which uses collective coordinates of QMFT:

- The mass and charge asymmetries $\eta = \frac{(A_1 - A_2)}{(A_1 + A_2)}$ and $\eta_z = \frac{(Z_1 - Z_2)}{(Z_1 + Z_2)}$.
- Deformations $\beta_{\lambda i}$, orientations θ_i of two fragments.
- Relative separation co-ordinate R.

For the ground state decay (T=0, $\ell=0$) of nucleus, the decay constant λ_{PCM} is defined as

$$\boldsymbol{\lambda_{PCM}} = \frac{\ln 2}{T_{1/2}} = \nu_0 P_0 P$$

Using the partial wave analysis, for the hot and rotating (T≠0 and $\ell \neq 0$) CN, the decay cross-section is defined as

$$\boldsymbol{\sigma_{DCM}} = \frac{\pi}{k^2} \sum_{\ell=0}^{\ell_{max}} (2\ell + 1) P_0 P \; ; \; k = \sqrt{\frac{2\mu E_{C.M}}{\hbar^2}}$$

Methodology

The preformation probability is given by

$$P_0 = |\psi_R(\eta(A_i))|^2 \sqrt{B_{\eta\eta}} \frac{2}{A^*_{CN}}$$

which we get by solving Schrödinger equation in η-coordinates

$$\left\{-\frac{\hbar^2}{2\sqrt{B_{\eta\eta}}}\frac{\partial}{\partial\eta}\frac{1}{\sqrt{B_{\eta\eta}}}\frac{\partial}{\partial\eta} + V_R(\eta)\right\}\Psi_R^{(\nu)}(\eta) = E_R^{(\nu)}\Psi_R^{(\nu)}(\eta)$$

Here $V_R(\eta, T)$ is the fragmentation potential and is defined as:

$$V_R(\eta, T) = \sum_{i=1}^{2}\left[V_{LDM} + \sum_{i=1}^{2}[\delta U_i]e^{\left(-\frac{T^2}{T^2}\right)}\right] + V_C\left(R, Z_i, \beta_{\lambda i}, \theta_i, T\right) + V_P\left(R, A_i, \beta_{\lambda i}, \theta_i, T\right) + V_\ell\left(R, A_i, \beta_{\lambda i}, \theta_i, T\right)]$$

V_C, V_P and V_ℓ are respectively the temperature dependent Coulomb, nuclear proximity and angular momentum dependent potentials.

P is the penetrability, refers to the R-motion, calculated by the WKB approximation

$$P = \exp[-\frac{2}{\hbar}\int_{R_a}^{R_b}\{2\mu\left[V(R) - Q_{eff}\right]\}^{1/2}dR]$$

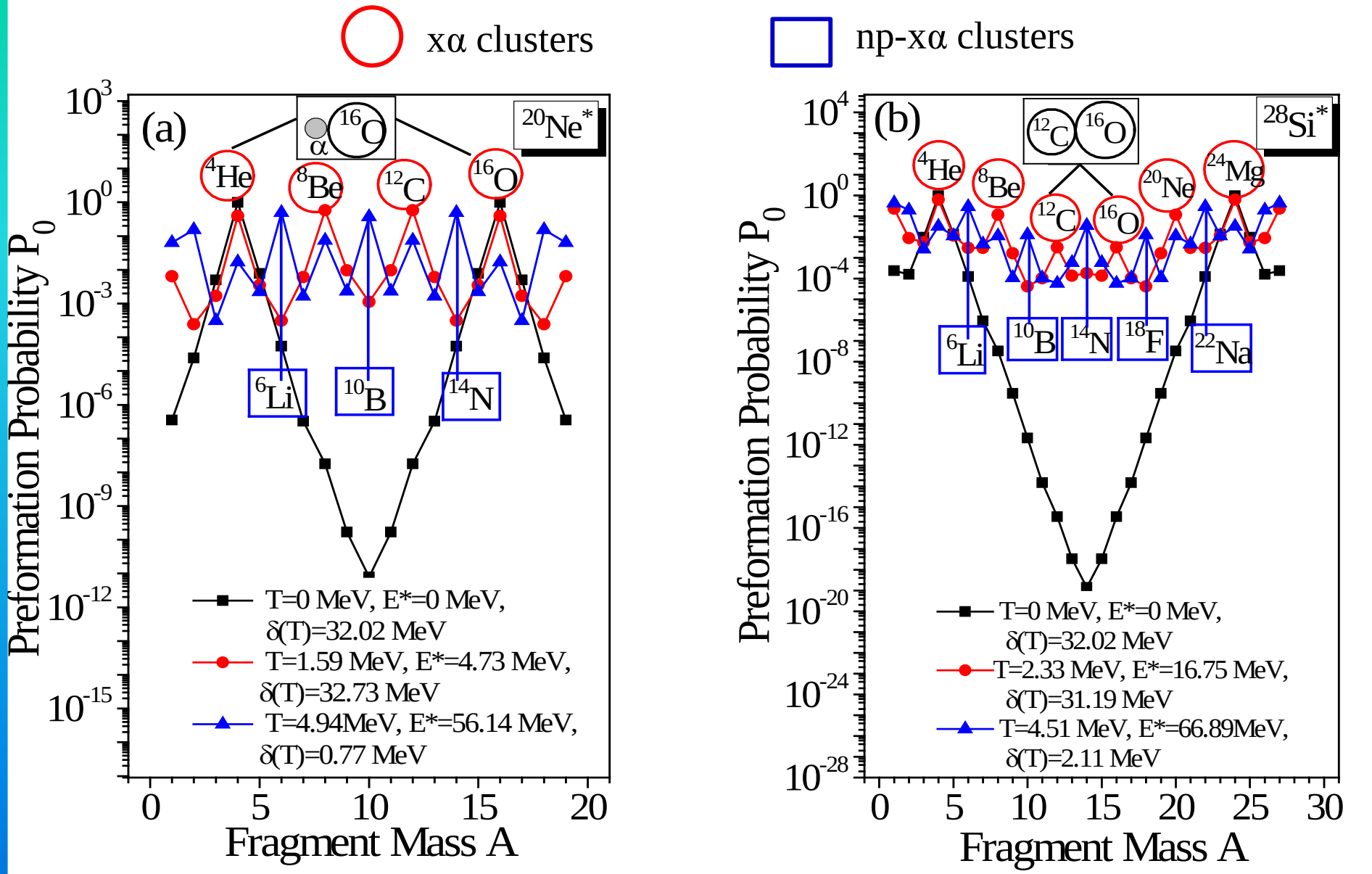

Fig1: Preformation profile of alpha conjugate system (a)$^{20}Ne^*$ (b)$^{28}Si^*$ at zero energy, resonant energy [K. Ikeda et al., Prog. Theor. Phys. (Suppl.) E 68, 464 (1968)] and experimental available energy [M. M. Coimbra et al., Nucl. Phys. A 535, 161 (1991)]

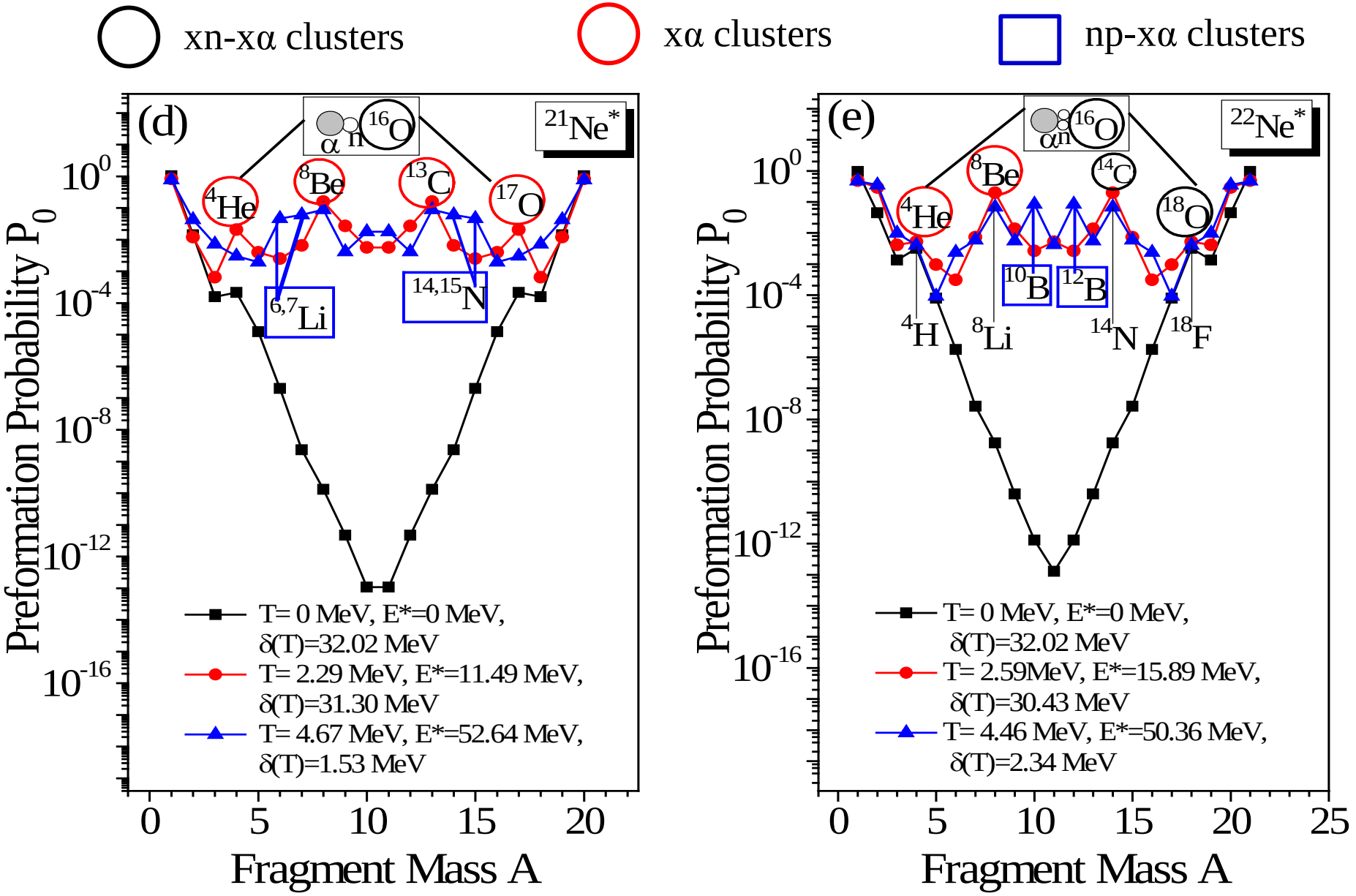

Fig2: Preformation profile of non-alpha conjugate system (a)$^{21}Ne^*$ (b)$^{22}Ne^*$ at zero energy, resonant energy [W. Von Oertzen et al., Eur. Phys. J. A 11, 403 (2001)] and experimental available energy [M. M. Coimbra et al., Nucl. Phys. A 535, 161 (1991)]

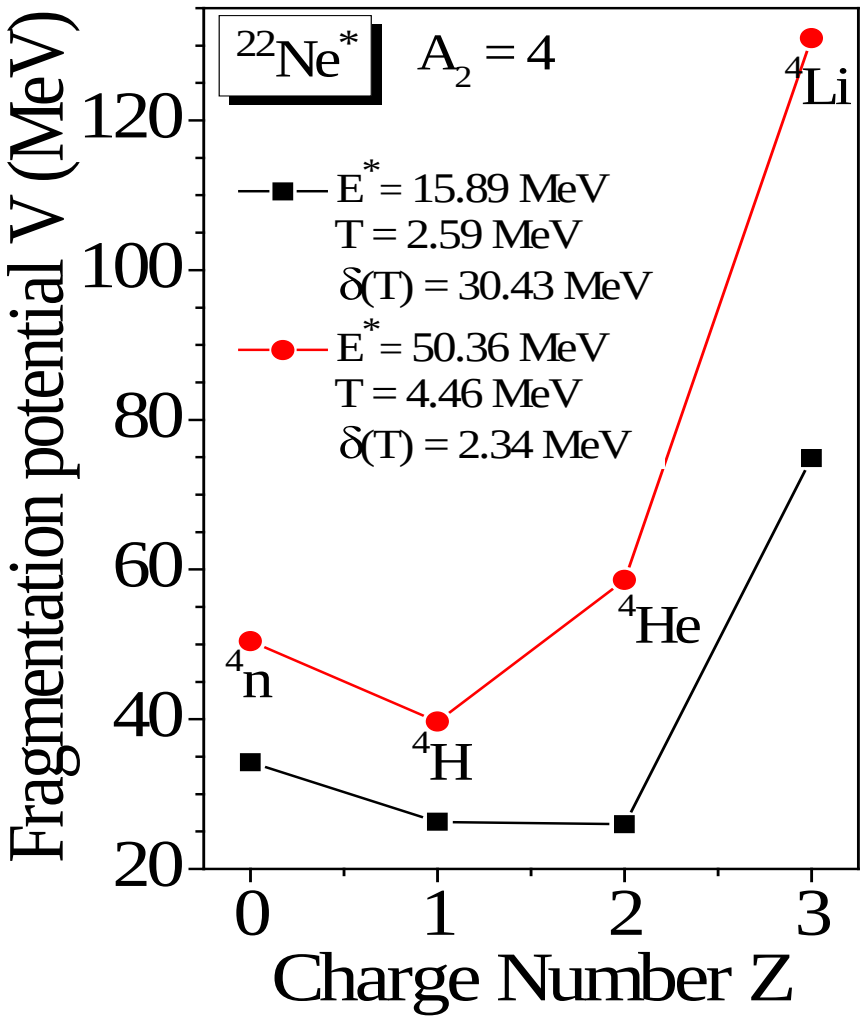

➢At resonant excitation energies (given by Ikeda) xα type and nx-nα clusters appear while at experimental available energy, np-xα type clusters also appear.

➢Thus the temperature dependent pairing energy plays an important role in clustering.

❖For $^{22}Ne^*$, *the clusters changes at* higher excitation energy of 15.89 MeV. This happens because of the change in Z-distribution with increasing temperature as shown in the figure here.

Fig3: Variation of the fragmentation potential V with fragment charge Z for A_2=4 fragment, for the decay of non-α conjugate system $^{22}Ne^*$ at T-values of their corresponding excited resonant state and the experimentally available excited state [M.M. Coimbra et al., Nucl. Phys. A 535, 161 (1991)].

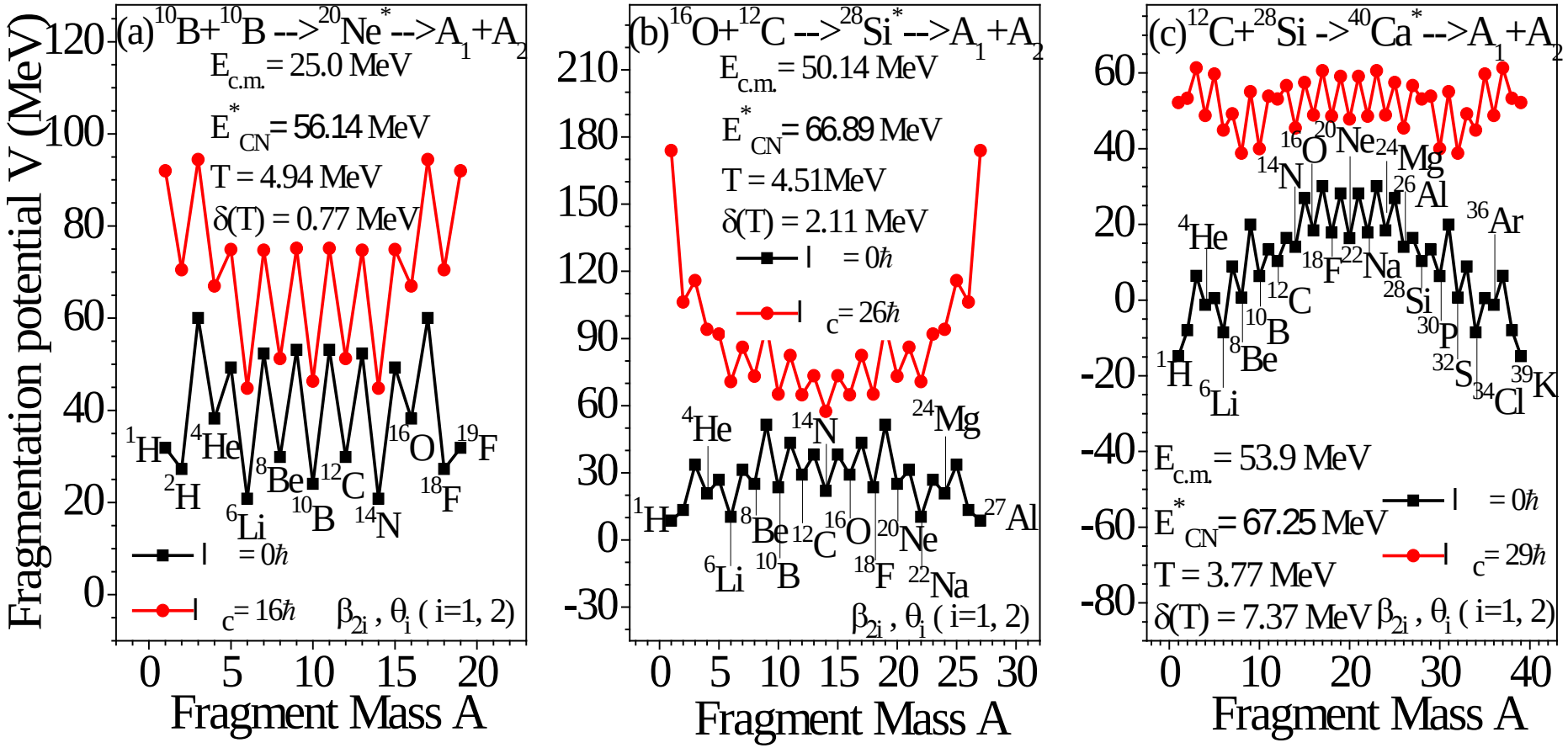

Fig.4: Variation of fragmentation potential V with fragment mass A for the decay of α-conjugate systems (a) $^{20}Ne^{*}$ (b) $^{28}Si^{*}$ and (c) $^{40}Ca^{*}$

- For $^{20}Ne^{*}$, at $\ell=0\hbar$ the LPs are in strong competition with IMFs but at $\ell=\ell c$, the binary symmetric decay (^{10}B) is in strong competition with neighboring IMFs (^{6}Li, ^{14}N).
- For $^{28}Si^{*}$, at $\ell=0\hbar$ the LPs are more energy minimized compared to IMFs but at $\ell=\ell c$, the binary symmetric decay (^{14}N) is strongly competes with neighboring IMFs (^{12}C, ^{16}O).
- For $^{40}Ca^{*}$, at $\ell=0\hbar$ the LPs are more energy minimized compared to IMFs but at $\ell=\ell c$, the IMFs (^{8}Be, ^{10}B) are more favorable than the binary symmetric decay (^{20}Ne).

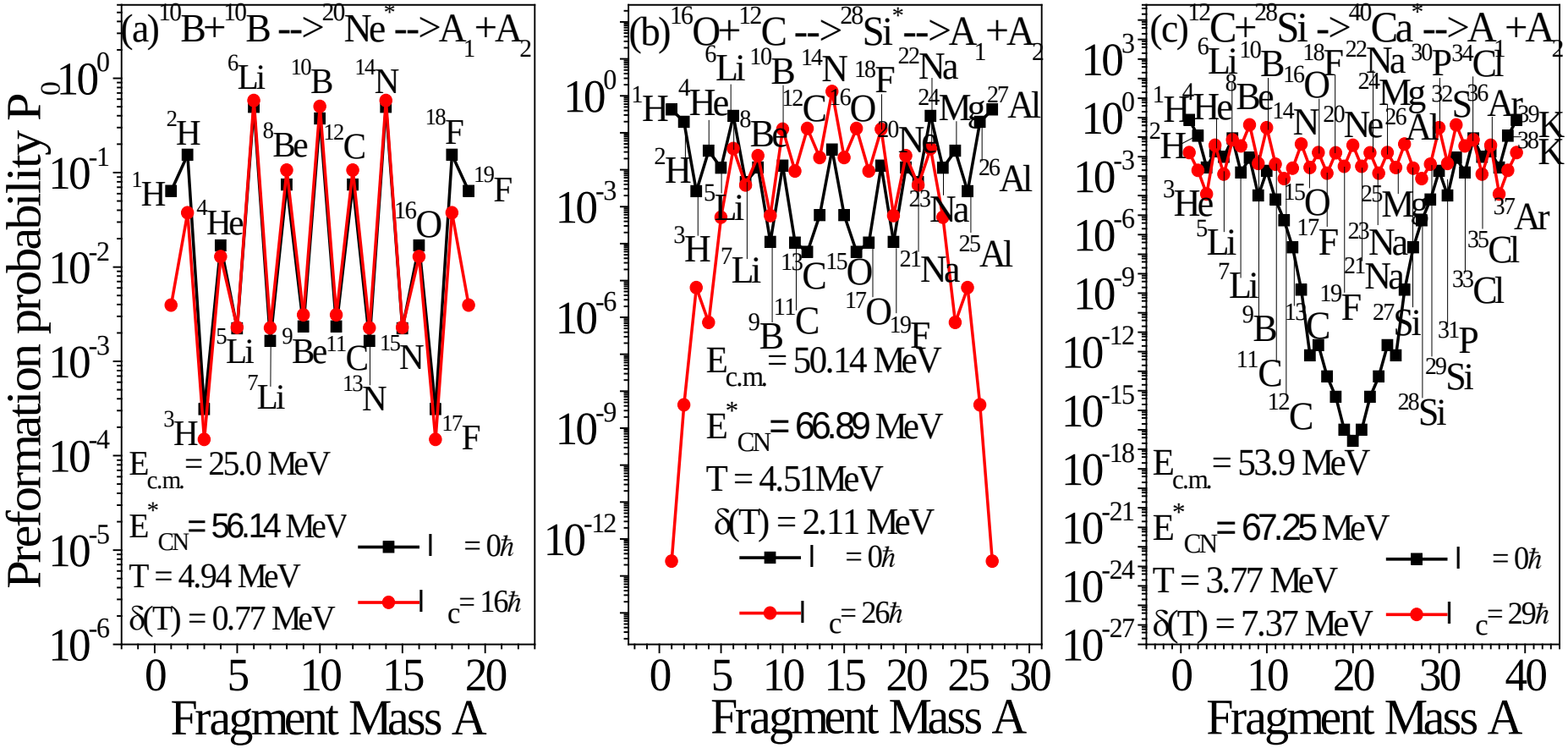

➢ **^{20}Ne* *system clearly demonstrate* the probable binary symmetric cluster configuration with the *IMF, ^{10}B (2α+p+n) at higher T-value* showing the large preformation yield, as observed also in RMFT for intrinsic excited states of ^{20}*Ne* [P. Arumugam et al, PRC 71, 064308 (2005)], *and also for the calculations within formalism* of EDF for ^{20}Ne [J. P. Ebran et al., Nature (London) 487, 341 (2012)].**

➢ ^{28}Si* *system at different T-values, present* the most probable binary symmetric cluster configuration with *IMF ^{14}N (3α+p+n) at higher T-value show*ing the largest preformation yield in comparison to lower T-values. The *α-clusters ^{16}O and ^{20}Ne*, have strong competition from ^{18}F (*4α +p+n)* and ^{22}Na (*5α +p+n) respectively.*

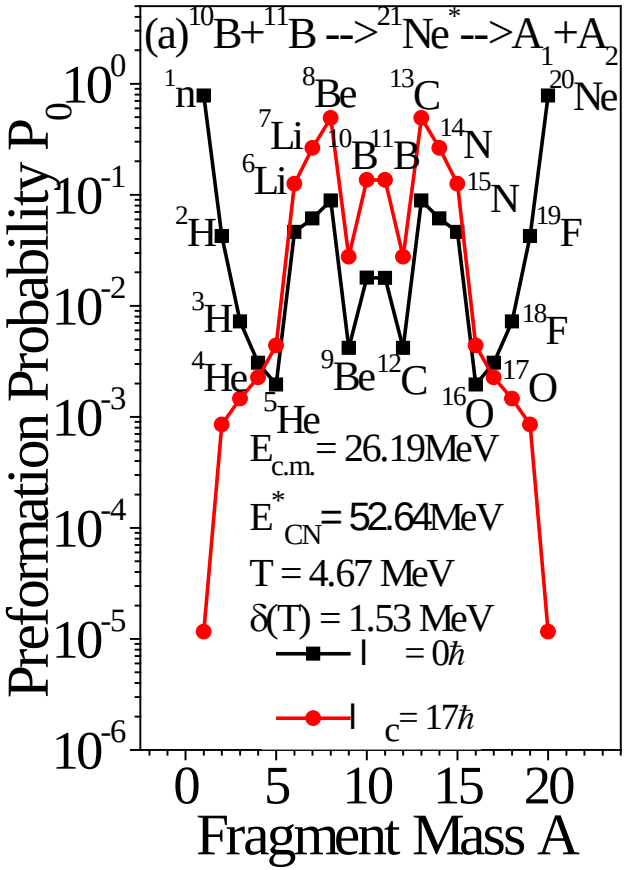

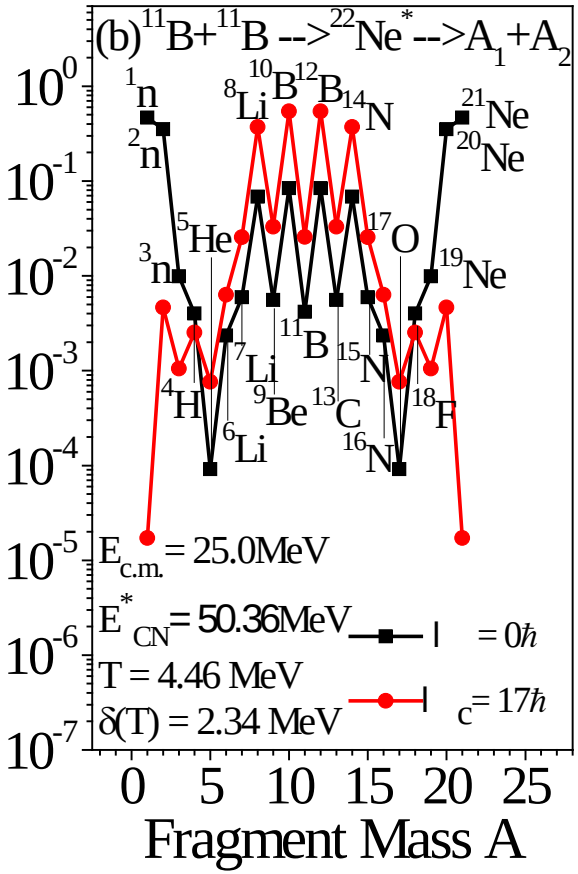

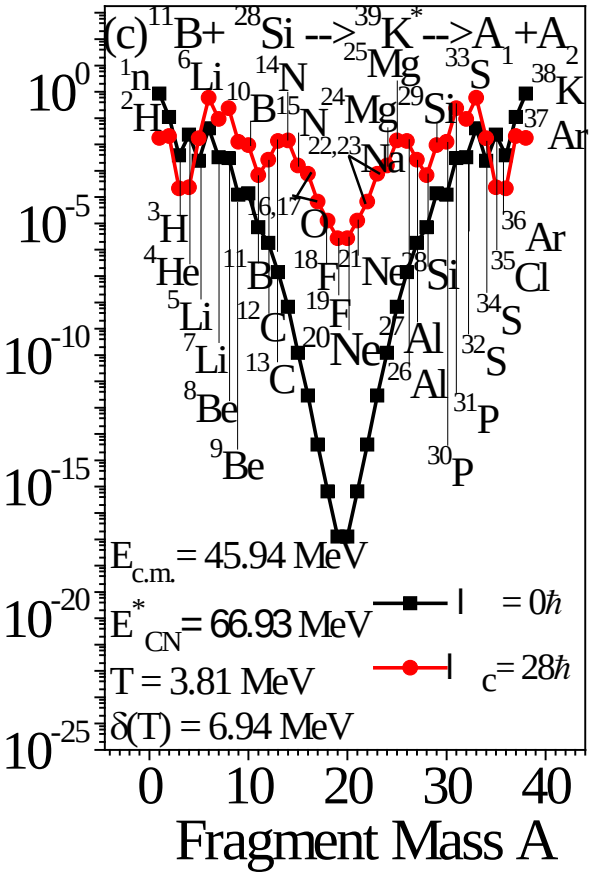

❖For N≠Z composite system $^{21}Ne^{*}$ demonstrate that the ^{13}C (3α+n) cluster is still dominant at higher T-value with competing binary near symmetric cluster configuration with the IMFs ^{10}B (2α+p+n) and ^{11}B (2α+p+2n) and ^{17}O (4α+n) cluster configuration is now not favored. Other clusters/ IMFs ^{14}N (3α+p+n) and ^{15}N (3α+p+2n)are strongly competing with other new possibilities.

❖For $^{22}Ne^{*}$, non-α cluster ^{14}C is replaced by the IMF ^{14}N (3α+p+n) competing strongly with the binary decay. The IMF ^{15}N (3α +p+2n), ^{16}N (3α+p+3n) and ^{18}F (4α+p+n) are also having small maxima. Note that ^{18}O (4α+2n) is replaced by ^{18}F (4α+p+n) at higher excitation energies.

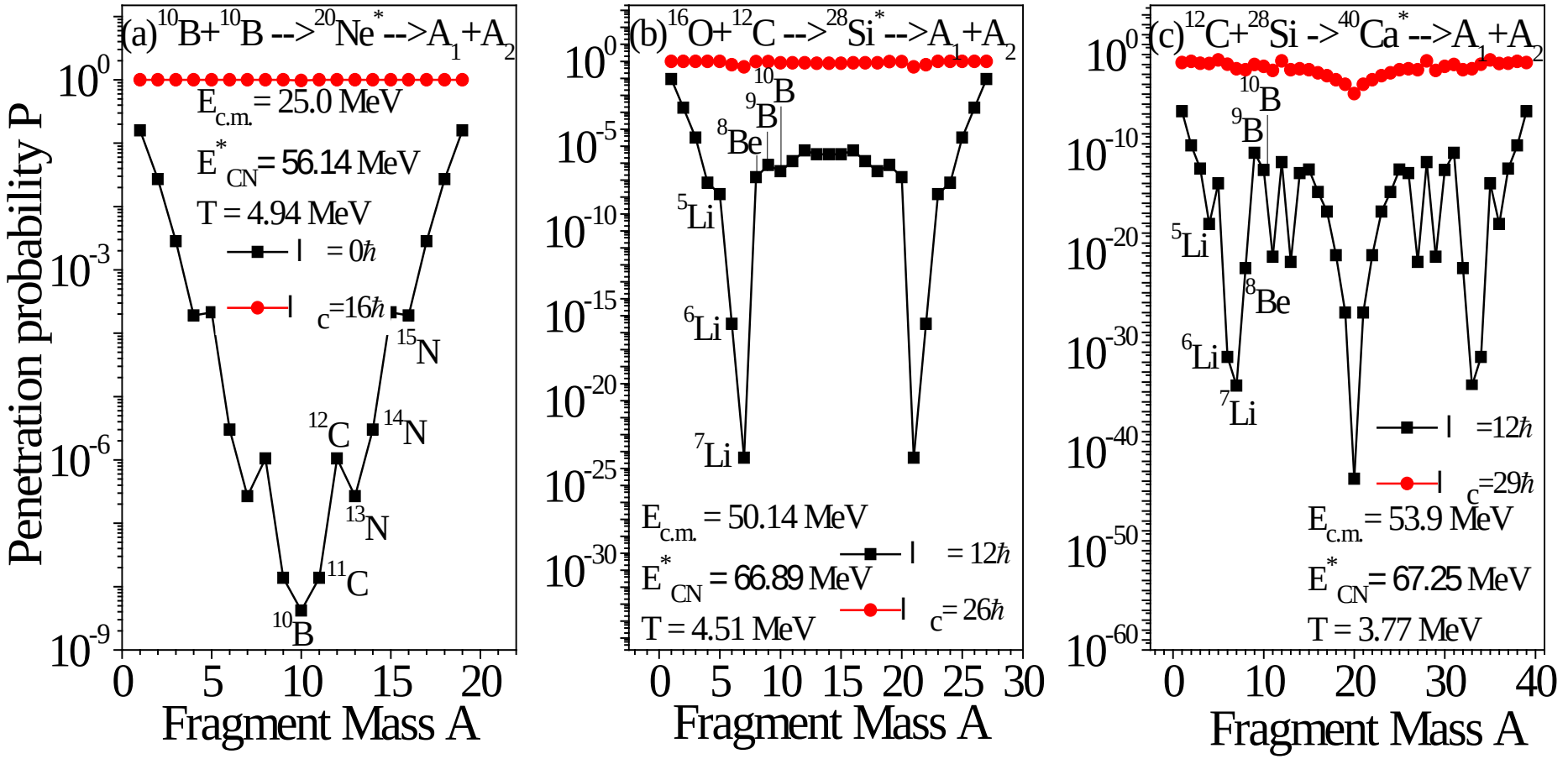

Fig7: Variation of penetration probability (P) with cluster mass the decay of α-conjugate systems (a) $^{20}Ne^{*}$ (b) $^{28}Si^{*}$ and (c) $^{40}Ca^{*}$

➢ At $\ell = \ell_c$, the Penetrability approaches 1 while at low angular momentum in case of (a)$^{20}Ne^{*}$, the ^{10}B cluster is having the least P while it is preformed strongly and $^{11,12}C$ and $^{13,14,15}N$ have the higher value of P.

➢In case of (b) $^{28}Si^{*}$ at low angular momentum, the ^{7}Li has the least P and other clusters $^{5,6}Li$, ^{8}Be, $^{9,10}B$ have higher P.

➢In case of (c)$^{40}Ca^{*}$ also, at low angular momentum, the ^{7}Li has a less P-value in comparison to $^{5,6}Li$, ^{8}Be and $^{9,10}B$, whereas the ^{20}Ne cluster is having least P although it has high value of P_0.

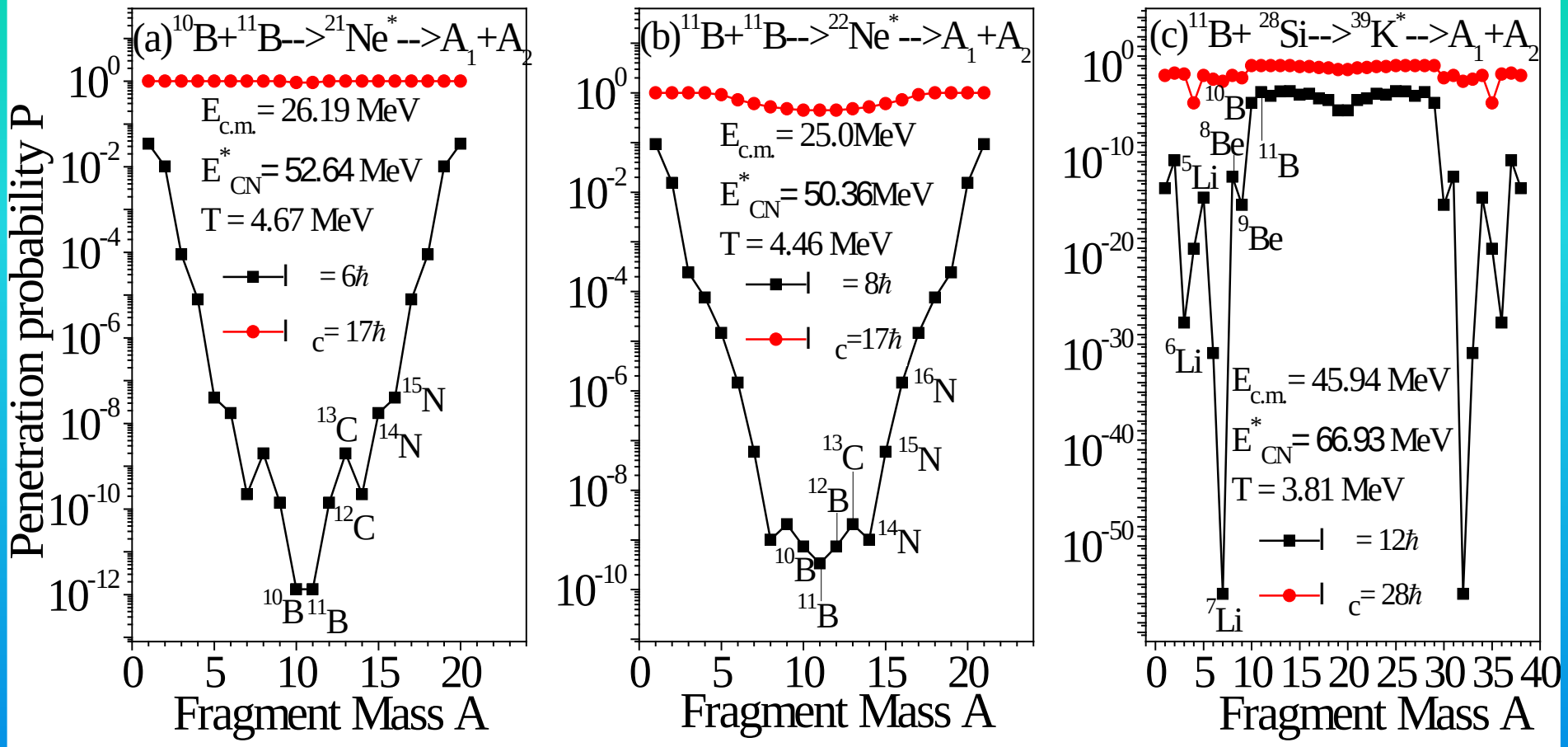

Fig8: Variation of penetration probability (P) with cluster mass the decay of non-α conjugate systems (a) $^{21}Ne^{*}$ (b) $^{21}Ne^{*}$ and (c) $^{39}K^{*}$

$E_{c.m.}$ (MeV)	E^*_{CN} (MeV)	T (MeV)	ℓ_c ($\hbar$)	ΔR (fm)			σ^{DCM}_{FF} (mb)			σ^{Expt}_{IMFs} (mb)			σ^{emp}_{DIO} (mb)		
				Z=5	Z=6	Z=7	Z=5	Z=6	Z=7	Z=5	Z=6	Z=7	Z=5	Z=6	Z=7
							$^{10}B+^{10}B \rightarrow ^{20}Ne^*$								
12	43.14	4.35	12	2.118	2.2	2.171	77.37	48.33	312.73	77.37	192.90	313.25	—	144.57	—
15	46.14	4.50	13	2.13	2.2	2.14	115.56	57.45	337.98	115.01	427.10	482.41	—	369.65	144.43
20	51.14	4.72	15	2.112	2.10	1.9	214.69	70.75	275.18	214.33	376.40	334.83	—	305.65	59.65
24	55.14	4.90	16	2.1	2.0	1.8	254.56	62.13	234.79	268.70	472.06	247.33	14.14	409.93	12.54
25	56.14	4.94	16	2.12	2.02	1.781	252.42	60.89	205.72	303.0	510.75	205.33	50.58	449.86	—
$E_{c.m.}$ (MeV)	E^*_{CN} (MeV)	T (MeV)	ℓ_c ($\hbar$)	ΔR (fm)			σ^{DCM}_{FF} (mb)			σ^{Expt}_{IMFs} (mb)			σ^{emp}_{DIO} (mb)		
				Z=3	Z=4	Z=5	Z=3	Z=4	Z=5	Z=3	Z=4	Z=5	Z=3	Z=4	Z=5
							$^{16}O+^{12}C \rightarrow ^{28}Si^*$								
50.14	66.89	4.51	26	1.223	1.542	1.585	17.06	12.72	38.34	42.68	14.20	60.28	25.62	1.48	21.94
53.57	70.32	4.62	26	1.24	1.56	1.61	16.79	11.86	37.38	44.12	17.32	63.95	27.33	5.46	26.57
62.14	78.89	4.92	26	1.31	1.625	1.67	16.56	10.98	34.24	68.34	21.53	83.31	51.78	10.55	49.07
68.57	85.32	5.08	25	1.47	1.75	1.792	20.36	11.58	32.02	95.16	33.13	126.48	74.80	21.55	94.46
$E_{c.m.}$ (MeV)	E^*_{CN} (MeV)	T MeV)	ℓ_c ($\hbar$)	ΔR (fm)			σ^{DCM}_{FF} (mb)			σ^{Expt}_{FF} (mb)					
				Z=3	Z=4	Z=5	Z=3	Z=4	Z=5	Z=3	Z=4	Z=5			
							$^{12}C+^{28}Si \rightarrow ^{40}Ca^*$								
53.90	67.20	3.77	29	1.14	1.14	1.34	4.08	2.81	3.82	$3.7^{+5.4}_{-1.7}$	$2.7^{+4.1}_{-1.2}$	$3.4^{+5.1}_{-1.5}$			

❖In particular case of BSD i.e. Z=5, for $^{20}Ne^*$ *the ff is the decay* mode up to $E_{c.m.}$=*24 MeV, afterwards* the DIO starts competing with ff. For Z=6,7 case, the ff and DIO shows competition.

❖In case of $^{28}Si^*$ with increase of energy, ff contribution remains almost same while the % contribution of DIO shows increase. The % contribution of DIO is maximum near the entrance channel(i.e. Z=5).

$E_{c.m.}$ (MeV)	E^*_{CN} (MeV)	T (MeV)	ℓ_c ($\hbar$)	ΔR (fm) Z=5	Z=6	Z=7	σ^{DCM}_{FF} (mb) Z=5	Z=6	Z=7	σ^{Expt}_{IMFs} (mb) Z=5	Z=6	Z=7	σ^{emp}_{DIO} (mb) Z=5	Z=6	Z=7
							$^{10}B+^{11}B\rightarrow^{21}Ne^*$								
13.09	39.54	4.07	12	1.987	2.2	2.2	17.29	142.15	171.92	17.36	802.48	600.83	—	660.33	428.91
15.71	42.16	4.20	13	2.09	2.2	2.2	45.85	183.10	219.05	46.31	739.95	732.66	—	556.85	513.16
20.95	47.40	4.44	15	2.19	2.12	2.05	111.86	241.13	201.36	111.16	881.22	743.16	—	640.09	541.80
26.19	52.64	4.67	17	2.0	1.92	1.78	109.28	231.53	168.24	159.80	713.31	484.10	50.52	481.78	315.86
							$^{11}B+^{11}B\rightarrow^{22}Ne^*$								
12	37.36	3.87	12	1.75	2.2	2.2	3.93	13.82	80.86	3.99	288.33	80.43	—	274.81	—
15	40.36	4.02	14	1.782	2.2	2.11	30.29	25.12	166.86	30.26	378.54	166.30	—	353.42	—
20	45.36	4.25	15	1.86	2.2	2.02	61.17	19.46	142.56	61.09	493.31	220.10	—	473.85	77.54
24	49.36	4.42	17	1.73	1.96	1.81	82.14	14.91	130.49	82.21	537.27	298.91	—	522.36	168.42
25	50.36	4.46	17	1.765	2.0	1.82	88.70	15.16	124.63	88.49	560.68	410.86	—	545.32	286.23
$E_{c.m.}$ (MeV)	E^*_{CN} (MeV)	T MeV)	ℓ_c ($\hbar$)	ΔR (fm) Z=3	Z=4	Z=5	σ^{DCM}_{FF} (mb) Z=3	Z=4	Z=5	σ^{Expt}_{FF} (mb) Z=3	Z=4	Z=5			
							$^{11}B+^{28}Si\rightarrow^{39}K^*$								
45.94	66.93	3.81	28	1.11	1.33	1.936	9.20	6.23	2.96	$8.5^{+10.0}_{-5.8}$	$5.3^{+8.0}_{-2.3}$	$21.0^{+32.1}_{-9.2}$			
							$^{12}C+^{27}Al\rightarrow^{39}K^*$								
50.53	67.14	3.81	30	0.97	1.16	1.78	9.30	5.06	2.53	$8.5^{+10.6}_{-6.2}$	$4.2^{+5.8}_{-3.0}$	$9.^{+13.0}_{-5.2}$			

❖For $^{21}Ne^*$; for Z=5 the ff contribution increases with increase in energy while for Z=6,7 the ff shows increase with energy but at higher most energy the ff contribution decreases.

❖For $^{22}Ne^*$; for Z=5 ff is the decay mode up to $E_{c.m.}$=25 MeV. For Z=6,7 case, the ff and DIO shows competition.

❖For $^{39}K^*$; the ff cross-sections are well reproduced for the Z=3,4 while for Z=5 we are not able to obtain a good agreement with experimental data.

Conclusion

❖ QMFT supports [[PRC 95, 014611 (2017)], clustering in N=Z (^{20}Ne * and ^{28}Si *) and N≠Z (^{21}Ne* and ^{22}Ne *) nuclear systems at excitation energies corresponding to their respective decay thresholds/resonant-state energies for the 4α, ^{16}O cluster and non-α cluster ^{14}C (more so in ^{22}Ne* N≠Z composite system), supported by the Ikeda diagrams, taking into account the proper pairing strength in the temperature dependent liquid drop energies.

❖Within the DCM, we notice that at higher excitation energies in addition to xα (where x is an integer) type clusters from N=Z composite systems and xn-xα type clusters from N≠Z composite systems, np-xα type clusters are relatively quite dominant, with larger preformation probability due to the decreased pairing strength at higher temperatures in the liquid drop energies.

❖Also, the study reveals the presence of competing reaction mechanisms of compound nucleus (fusion-fission, FF) and of non- compound nucleus origin (deep inelastic orbiting, DIO) in the decay of very light mass composite systems $^{20;21;22}$Ne* and ^{28}Si * at different excitation energies.

❖The DIO contribution in the intermediate mass fragments (IMF) cross section σ_{IMF} is extracted for these composite systems, σ_{IMF} is given as the sum of FF cross section σ_{FF} and DIO cross section σ_{DIO}. The DCM calculated FF cross-sections $\sigma_{DCM}{}^{FF}$ are in good agreement with the available experimental data.


Thank You